DISLOCATION ELECTRON TOMOGRAPHY OF BOUNDARIES IN DEFORMED ALUMINIUM

Amuthan Ramar*, Satoshi Hata**,
Xiaoxu Huang***, Rafal E. Dunin Borkowski* and Grethe Winther***

* Center for Electron Nanoscopy, Technical University of Denmark, DK-2800 Kgs. Lyngby, Denmark
** Department of Engineering Sciences for Electronics and Materials, Kyushu University, Kasuga, Fukuoka 816-8580, Japan
*** Danish-Chinese Center for Nanometals, Materials Research Division, Risø National Laboratory for Sustainable Energy, Technical University of Denmark, DK-4000 Roskilde

ABSTRACT

Dislocation tomography has been applied to deformation-induced dislocation boundaries in tensile deformed aluminium. Using one diffraction vector a series of Scanning transmission electron microscopy (STEM) high-angle annular dark field (HAADF) images at a wide range of tilt angles has been acquired and reconstructed in three dimensions (3D). The data reveal the detailed dislocation arrangement wihtin a planar boundary and also the 3D shape of curved cell boundaries.

1. INTRODUCTION

Over the last 50 years transmission electron microscopy (TEM) has been a key technique to investigate dislocations and the way dislocations organise themselves spatially. However, the acquired images are two-dimensional projections of the 3D structure. Tilting of the TEM foil in the microscope can provide different projections. Based on such tilting 3D tomographic reconstruction of individual dislocations and dislocation networks is possible if the diffraction conditions are kept constant throughout the tilt series (Barnard, Sharp, Tong and Midgley 2006; Tanaka, Higashida, Kaneko, Hata and Mitsuhara 2008).

Bright-field or dark-field TEM using parallel beam illumination it is difficult to obtain uniform contrast of dislocations due to the sensitive change in diffraction contrast. Scanning transmission electron microscopy (STEM) using convergent beam illumination is less sensitive to the diffraction

constant and thickness contrast, such as thickness oscillation and fringes. It allows for large deviations from the exact Bragg condition, which facilitates good dislocation images from a tilting series (Sharp et al 2008, Barnard 2007). The present paper applies STEM dislocation tomography to reveal the dislocation arrangement within a planar dislocation boundary as well as the 3D morphology of dislocation cells in a deformed aluminium sample. The focus is on the technical challenges, which must be overcome to produce a good reconstruction. The method is demonstrated using single diffraction vector.

2. EXPERIMENTAL DETAILS

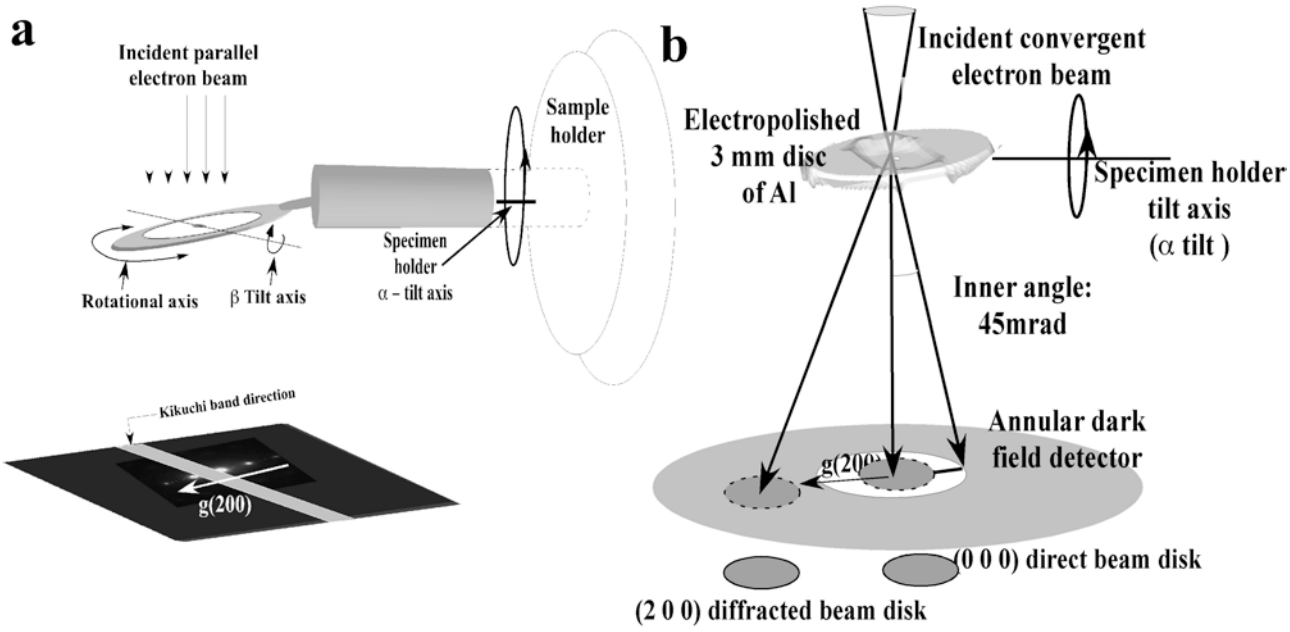

Fig.1 (a) Diffraction condition used for imaging and sample position across the tilt axis. (b) Schematic diagram of the geometry of the annular dark-field and diffraction disc of g(hkl)=200 (adapted from Tanaka, Higashida, Kaneko, Hata and Mitsuhara 2008)

The microscope used for the investigation is an FEI Titan Analytical TEM (A-TEM). The A-TEM is operated at 300kV and is equipped with a Field emission gun (FEG), monochromator and a probe C_S corrector. This microscope has a STEM, high-angle ADF (HAADF) and tomography observations.

The HATA (High Angles Triple Axis) holder (produced by Mel-Build) is used for the acquisition of the STEM tilt series. Using this holder it is possible to tilt the sample up to ±83º in alpha (α), ±7º in beta (β) inside the TEM and ±5º around the rotational axis as shown in the fig.1a. The beta tilt axis falls perpendicular to the sample holder tilt axis. More detailed information about the holder is found else where (www.melbuild.com). Fig.1a schematically represents the sample and the holder position in the microscope, for the given diffraction condition where the arrow on the diffraction pattern shows the alpha tilt axis of the holder and gray band drawn in the lower image represents the Kikuchi band which is a guide adjust to the diffraction condition as well as the α tilt axis. The

diffraction vector was maintained close to *g (hkl)* = 200 during the acquisition of the STEM images by adjusting the [100] direction of the sample parallel to the alpha tilt axis of the holder by means of the beta tilt and the rotational sample stage. An ADF-STEM tilt series was acquired with an alpha tilt range from -60° to +60° with a 2º interval. The acquisition of the tilt series is schematically shown in Fig.1b.

The material to which the dislocation tomography technique is applied here is a 99.5% pure aluminium polycrystal with a grain size of 75 µm, which had been elongated 25% in uniaxial tension. The TEM foil is prepared as described by (Christiansen, Bowen and Lindbo 2002) and the plane of the foil contains the tensile axis. The morphology of the grain subdivision by means of dislocation boundaries in this and similar materials has been extensively studied, revealing three basic types of overall structures (Huang and Winther 2007). The present experiment was conducted for a grain containing parallel extended planar dislocation boundaries, in between which randomly oriented dislocation cell boundaries are observed.

3. RESULTS

Fig. 2 shows a TEM bright field image of the dislocation boundaries investigated here. Two representative regions were selected for dislocation tomography: A planar boundary as marked by the circle in Fig. 2 and the region in the square that contains cell boundaries. The latter region has been reconstructed in 3D.

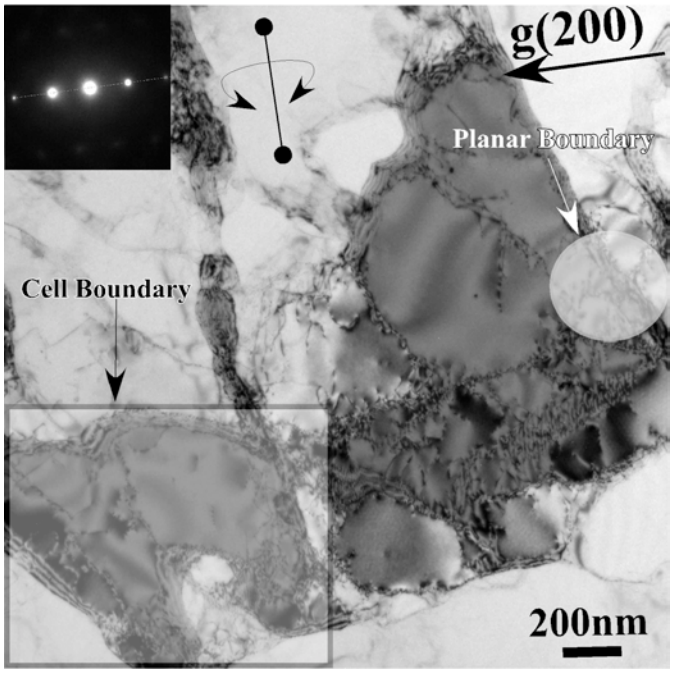

Fig. 2: TEM bright field image of the deformed Al showing a deformation induced structure of curved cell boundaries and planar boundaries.

Fig.3 shows the HAADF STEM tilt series image of the planar boundary marked by the circle in Fig.2 using g (200). The diffraction condition is the two beam condition which is shown as an insert at 0º tilt. The tilt series gives a 3D view of the boundary, which is almost perpendicular to the beam direction at -44º and parallel to the beam at +48º, where the planar boundary is viewed almost edge-on. The straightness of the boundary in the latter image shows that the boundary is almost perfectly planar with only a little curvature. The image taken at alpha= -44º shows that the boundary is planar in the sense that it is extended in two dimensions, the one lying in the plane of the TEM foil being larger than the other dimension, which may, however, possibly be limited by the foil thickness.

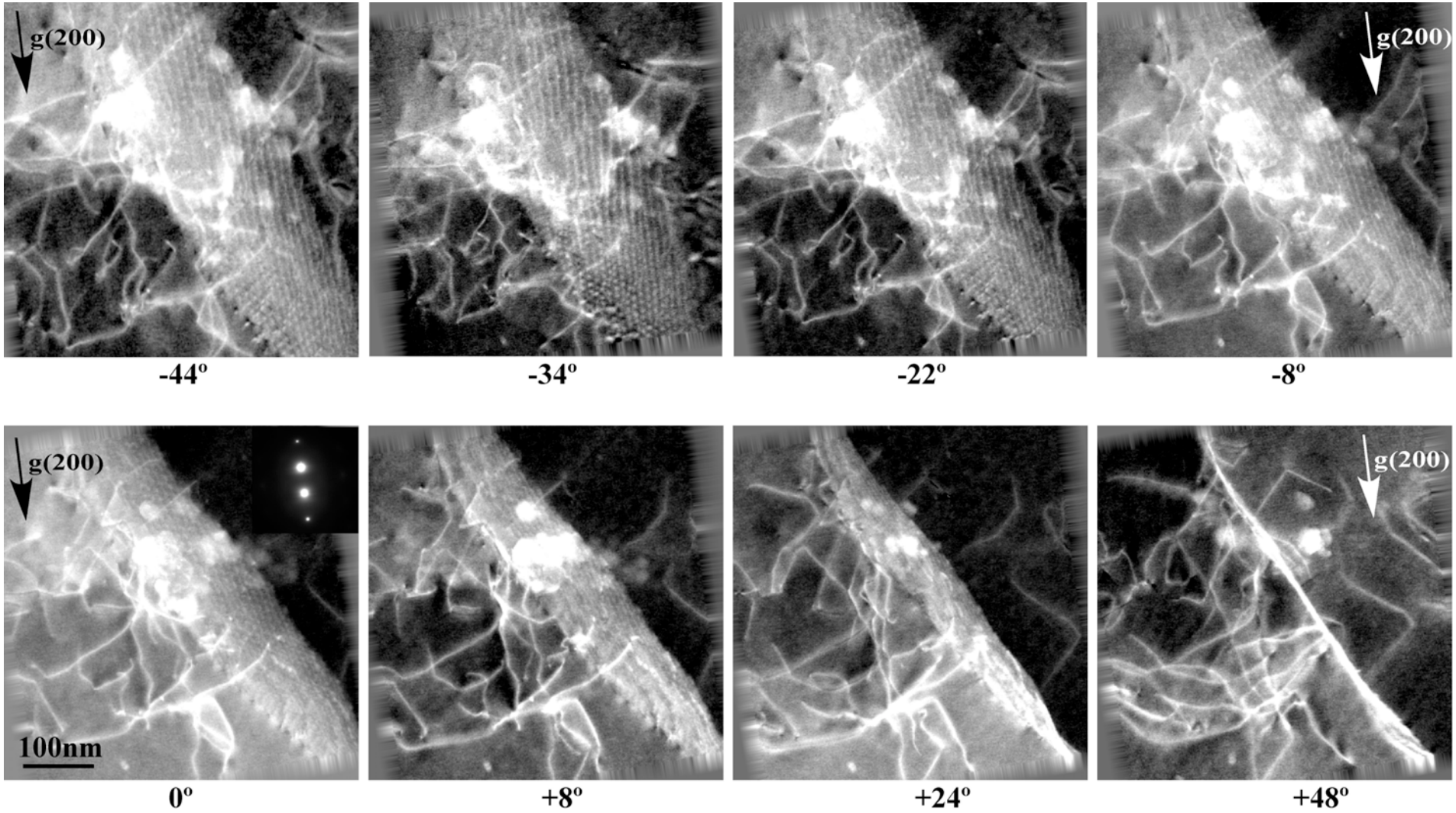

Fig. 3 shows a part of HAADF STEM tilt series of the planar boundary marked in Fig. 2 (in circle) taken at different alpha tilt angles using the two-beam condition for g (200).

The images reveal one clear set of parallel regularly spaced dislocation lines in the planar boundary. A number of dislocations do not lie in the plane of the boundary and some appear attached to the boundary. The density of such dislocations is higher on the left side of the boundary. The dislocations do not seem to penetrate the boundary. These 3D dislocation arrangements can be confirmed by stereo pair observation (e.g. 0º and 8º images).

Fig. 4 (a-c) shows a part of the ADF STEM tilt series of the structure shown in the square in Fig.2 taken at different alpha tilt angles, namely -34º, 0º and +12º, using g(200). Fig.4d-f shows different views of the 3D reconstruction of the dislocation cell boundaries. The 3D reconstruction was carried out with the FEI 3D-inspect software using SIRT (Simultaneous Iterative Reconstruction Technique) and the 3D imaging was performed using the Avizo software. The 3D reconstruction not only reveals highly curved boundaries but also an almost planar boundary segment in the lower left corner. The individual dislocations are, however, somewhat blurred in the reconstruction.

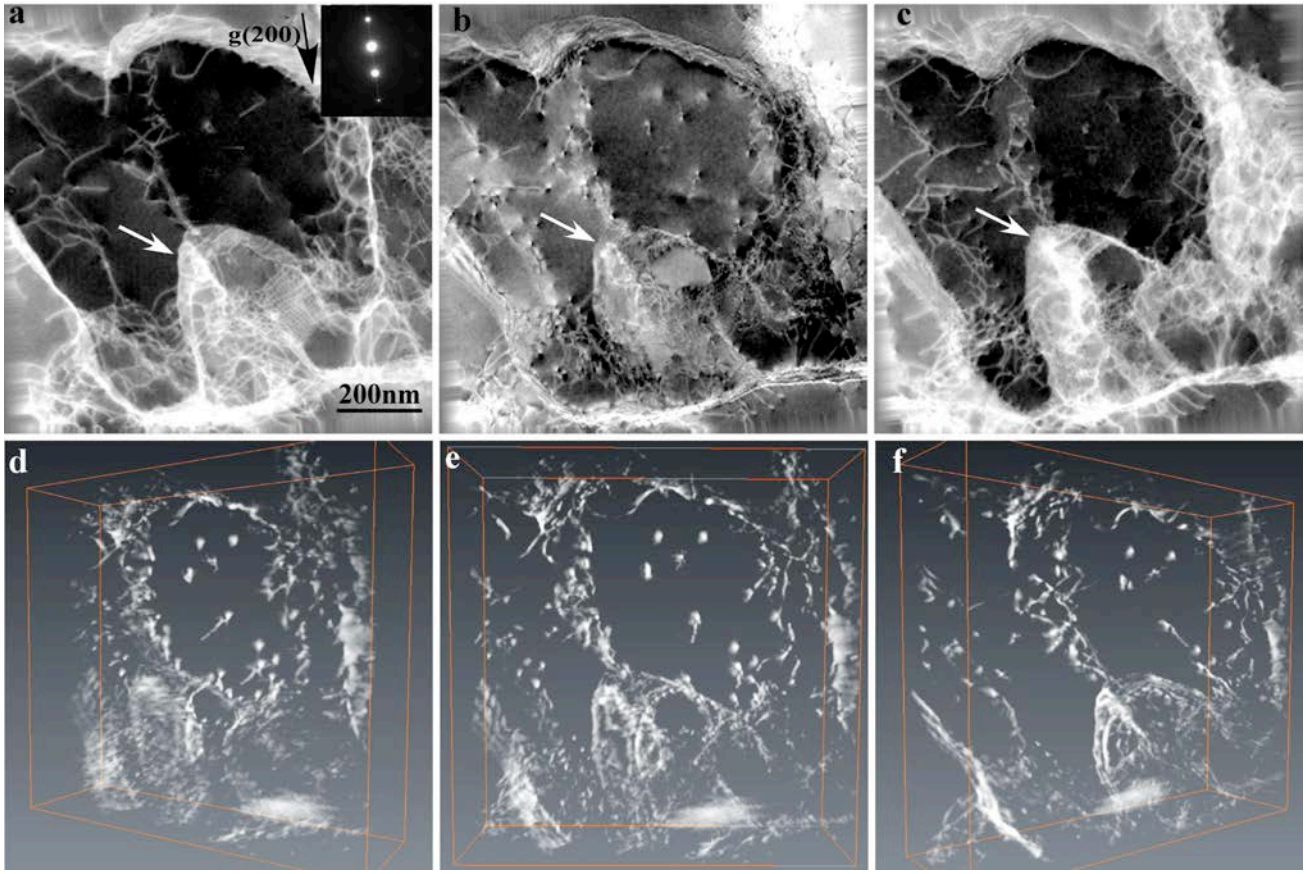

Fig. 4: (a-c) A part of the ADF STEM tilt series of the dislocation cell boundaries inside the square in Fig. 2 using g (200) at alpha tilt angles of -34º, 0º and +12º. (d-f) 3D reconstruction viewed from different sides.

Fig. 5 (a-b) shows a part of the HAADF STEM tilt series of the dislocation cell structure shown in the square in Fig.2 and marked with arrows in fig.4 taken at different alpha tilt angles, namely -32º and +8º, using g(200), which is an characteristic of dislocation arrangement upon tensile deformation in aluminium (Al). Fig.5 c,d shows different views of the 3D reconstruction of the boundaries. The regions marked with the arrow in Fig.5, is a cell boundary that is orientated

perpendicular to the electron beam, where we could see clearly two sets of dislocations which are perpendicular to each other.

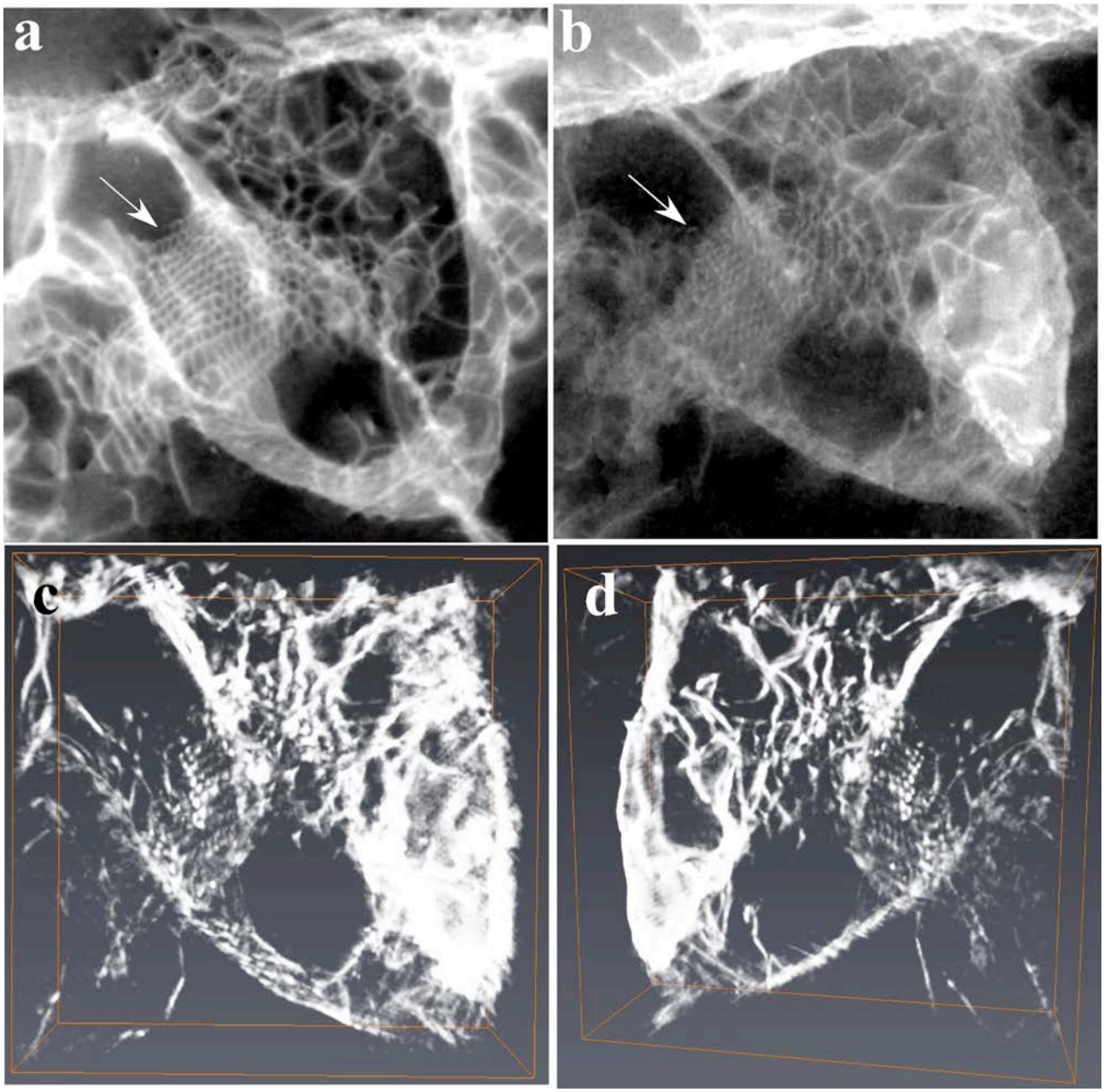

Fig. 5: a-b) Series of the HAADF images of the dislocation cells and its from Fig. 4 using g (200) at alpha tilt angles of -32º and +8º, c-d) 3D reconstruction viewed from different sides.

4. DISCUSSION

In aluminium, the dislocations are expected to have Burgers vectors of the $\boldsymbol{b}$ = ½ **<110>** type. Twelve such b's are possible and only those for which $g \cdot b \neq 0$ are visible in the images. Using g(200) dislocations with only eight b's are visible and it is therefore possible that some dislocations are not revealed in the present experiment. To reveal all dislocations of the **b=½ <110>** type, a possibility

is to use two diffraction vectors for example g (200) and g (220) in the [001] zone axis. It is achievable to obtain two tilt series with g (200) and g (220) at [001] using the current holder by rotating the sample 45º in the plane of the foil in between the tilt series. However, to unambiguously identify the Burgers vectors, the use of several diffraction vectors is necessary. In general, the dislocations forming a cell boundary or a planar boundary have fewer than six b's. A proper selection of diffraction vectors will allow all the dislocations to be resolved and identified.

Fig.5 shows the clear dislocation arrangements at the deformation cell structure. There are two perpendicular sets of dislocations, which should likely have the burgers vector of **b = ½ <110>** type. Both the sets of dislocations are clearly visible at -32º and where as only one set is well defined at +8º. The dislocation density varies on either side of the cell. However, it is found that the dislocation density in between the cell boundary is much higher than the dislocation in between the planar boundaries.

At the bottom of the 3D reconstruction in Fig. 4d-f a cloud-like structure is seen, which doesn't appear in the original individual images (Fig. 4a-c). This could be an artifact upon reconstruction. Such an artifact could be due to a rapid change in the diffraction contrast across the image at certain tilt angles if the sample passes through different zone axes, where other g vectors may become partially excited. Where as in Fig.5, the dislocations looks like more broadened rather to be sharp lines. This could be due to the changes in the contrast across the images.

The 3D reconstruction methods need further improvement as the current reconstruction shows some artefacts, in particular blurring of the individual dislocation lines. As an initial step to improve the reconstruction, the imaging condition could be improved. Application of filters to the original images and optimization of the contrast is expected to decrease the artefacts. However, there is probably a need for a better algorithm / program to reconstruct lines, in particular curved ones.

CONCLUSIONS AND OUTLOOK

Dislocation tomography is a challenging but promising technique for studies of complex deformation induced dislocation boundaries in metals. The main challenges lie both in the demanding experimental conditions needed to obtain tilt series of high quality images and in the subsequent 3D reconstruction. When successful the technique not only allows studies of the dislocation arrangement in the boundaries but also of the interaction between a boundary and dislocations not yet fully incorporated in the boundary. Such studies are important to understand the mechanisms behind boundary formation and evolution.

ACKNOWLEDGEMENTS

XH and GW gratefully acknowledge support from the Danish National Research Foundation and the National Natural Science Foundation of China (Grant No. 50911130230) for the Danish-Chinese Center for Nanometals, within which part of this work was performed.

This work was supported in part by the Grants-in-Aid from the Japan Society for the Promotion of Science (JSPS) and the Grant-in-Aid from the Ministry of Education, Culture, Sports, Science and Technology (MEXT), Japan.

S. H. thanks H.Miyazaki (Mel-Build), S. Miyazaki (FEI), T. Kasama (DTU), M. Mitsuhara, K. Ikeda, H. Nakashima (Kyushu University) and Lionel C. Gontard (DTU) for their valuable supports and comments.

REFERENCES

Barnard, J., J. Sharp, J. Tong and P. Midgley (2006). Three-dimensional analysis of dislocation networks in GaN using weak-beam dark-field electron tomography. Philosophical Magazine 86: 4901.

Christiansen, G., J. Bowen and J. Lindbo (2002). Electrolytic preparation of metallic thin foils with large electron-transparent regions. Materials Characterization 49: 331-335.

Huang, X. and G. Winther (2007). Dislocation structures. Part I: Grain orientation dependence. Philosophical Magazine A 87: 5189-5214.

Tanaka, M., K. Higashida, K. Kaneko, S. Hata and M. Mitsuhara (2008). Crack tip dislocations revealed by electron tomography in silicon single crystal. Scripta Materialia 59: 901-904.

Mel-Build, Kyushu island, JAPAN, Web site: www.melbuild.com

Kaneko, K, K. Inoke, K. Sato, K. Kitawaki, H. Higashida, I. Arslan and P.A. Midgley, Ultramicroscopy 108 (2008) 210. Conventional HAADF STEM tomography

J.H.Sharp, J.S.Barnard, K.Kaneko, K.Higashida and P.A.Midgley (2008). Dislocation tomography made easy: A reconstruction from ADF-STEM images obtained using automated image shift correction. Journal of Physics: Conference series 126 : 012013

J.S.Barnard, J. Sharp, J.R.Tong and P.A.Midgley (2007). Electron tomography of dislocations. Microscopy and Microanalysis 13 (2): 150 – 151